Alignment of the CMS Muon System with the HIP Algorithm

Jim Pivarski, Karoly Banicz, Alexey Kamenev, Alexei Safonov

August 29, 2007

1 Introduction

The positions and orientations of CMS muon chambers must be well understood for accurate measurements of muon momentum, especially for muon tracks with energies on the order of 1 TeV [**?**]. In addition to monitoring these parameters with a dedicated apparatus [**?**], we will also measure the alignment using tracks identified by the chambers themselves using the HIP algorithm. This track-based alignment has several advantages, the most important being that tracks reveal the positions of the sensitive elements directly, rather than through the structure that supports them, and the precision on each degree of freedom is proportional to that which is needed for track reconstruction.

The fundamental difficulty in aligning any detector with the tracks it observes is that the process of fitting tracks depends on the assumed position of the detector. One immediate consequence of this circular dependence is that the global position of the whole detector can never be determined with tracks alone. Therefore, our emphasis will be on relative alignments of one system to another, usually the chambers of the muon system (barrel and endcap) relative to the silicon tracker, but also muon chambers relative to one another.

1.1 The HIP algorithm

The HIP algorithm (Hits and Impact Points, [**?**]) addresses the interdependence of track fitting with alignment by alternating between the two in an iterative approach. The alignment step is very simple: chambers are moved in such a way as to make the weighted mean of their residuals distribution zero before refitting. (A residual is the difference between the track's extrapolation to the detector surface, called the impact point, and the measured hit.)

To illustrate this method, let's consider the algorithm in a one-dimensional case. At each iteration, the correction to the x position of the chamber is equal to the weighted mean of the x residual distribution, negated.

$$\text{Alignment correction} = -\frac{b}{A} \pm \frac{1}{A} \text{ with } A = \sum_{\text{all hits}} \frac{1}{{\sigma_r}^2} \text{ and } b = \sum_{\text{all hits}} \frac{r}{{\sigma_r}^2}, \tag{1}$$

where r is the residual (track minus hit) and σ_r is its uncertainty, for each hit.

In general, each hit in the real detector measures one or two dimensions in its sensitive plane (residuals $\vec{r} = r_x$ and r_y with covariance matrix ${\sigma_r}^2$) which are transformed to the (at most) six-dimensional space of local alignment corrections $\vec{q} = x$, y, z, ϕ_x, ϕ_y, and ϕ_z through an (at most) 6×2 Jacobian matrix $(\partial q/\partial r)$. (We can fix degrees of freedom that are not well determined, reducing the dimensionality of the problem.) The alignment corrections still look like a weighted mean:

$$\text{Alignment corrections} = -\mathbf{A}^{-1} \cdot \vec{b} \ \pm \ \mathbf{A}^{-1} \tag{2}$$

where

$$\mathbf{A} = \sum_{\text{all hits}} \left(\frac{\partial q}{\partial r}\right) \left({\sigma_r}^2\right)^{-1} \left(\frac{\partial q}{\partial r}\right)^T \tag{3}$$

and

$$\vec{b} = \sum_{\text{all hits}} \left(\frac{\partial q}{\partial r}\right) \left({\sigma_r}^2\right)^{-1} \vec{r}. \tag{4}$$

Since the matrix inversions are at most 6×6, most of the computational effort in the HIP algorithm is spent re-fitting tracks and producing updated residuals distributions between iterations.

1.2 The geometry of the muon system

The muon system is composed of a barrel of drift tube chambers and two endcaps of cathode strip chambers surrounding all other CMS detectors (see Figure 1).

A drift tube is an anode wire in a cylindrical, gas-filled tube, held at high voltage with respect to the outer surface of the tube. It measures the distance of closest approach of a charged track to the wire through the time needed for electrons to drift from gas atoms, ionized by the track's passage, to the wire [**?**].

Drift tube chambers (DTs) are rectangular sandwiches of 8–12 layers of drift tubes. Each layer measures the intersection of the track with the layer plane in one dimension: x in local chamber coordinates for the first four layers (superlayer 1) and the last four layers (superlayer 2 or 3). Chambers with 12 layers (all but MB 4: see Figure 1) have a third superlayer in the middle that measures y in local chamber coordinates, being rotated a 90° angle with respect to superlayers 1 and 3. In global CMS coordinates, the DTs' local x corresponds roughly with $r\phi$, the polar angle around the beamline, and local y corresponds exactly with global z, the direction along the beamline. The layers are stacked in local z.

There are 250 DTs: 4 stations in global r times 5 wheels in global z times 12–14 sectors in global ϕ. (Only MB 4 has 14 sectors.)

A cathode strip is a band of conducting material painted on a layer plane, measuring the intersection of a track through that plane by comparing the charges collected on neighboring strips. In the cathode strip chambers (CSCs), 6 trapezoidal layers of cathode planes alternate with layers of anode wires. The strips measure the track intersection point along a dimension which is nearly collinear with local x: "nearly" because the strips fan from the narrow end of the trapezoid to the wide end, and only the central strip measures x exactly (see Figure 2). The wires measure the same intersection point in the local y direction. Just as for the DTs, local x corresponds roughly with $r\phi$ in the global CMS coordinate system, but for CSCs,

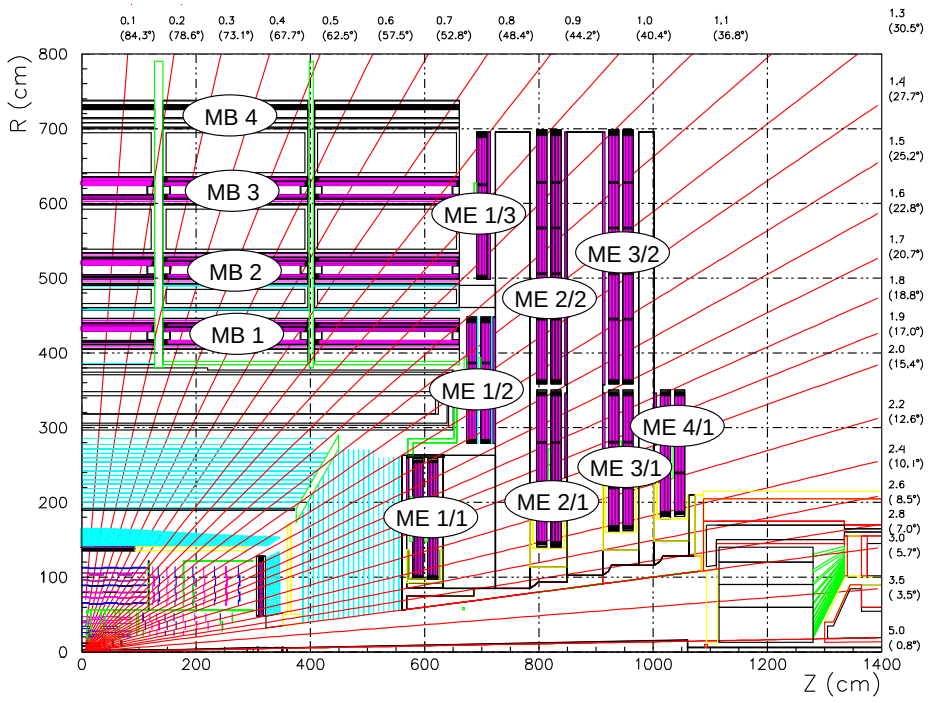

Figure 1: A quarter-view of CMS, highlighting the muon barrel (MB) and endcap (ME) stations.

local y corresponds roughly with global r. The CSC layers are also stacked in local z, but in decreasing order (layer 1 is "above" layer 6 in z).

For alignment purposes, there are 540 CSC chambers, not all of which are physically distinct. Chambers in ME 1/1 (see Figure 1) have a unique geometry: they are doubled (12 active layers) in such a way that each may be treated as two chambers [**?**]. In the geometry description used by track reconstruction, half of each double-chamber is said to belong to a new station, ME 1/4. We will use the same convention.

The intrinsic resolution of a DT hit (x or y) is approximately 300 μm [**?**]. The intrinsic resolution of a CSC hit can be as small as $\sim$200 μm in local x if the track intersection is between strips, $\sim$?? μm otherwise. (Strips are staggered from one layer to the next to guarantee that about half of the hits will have optimum precision in x.) Local y resolution is about 1 cm for CSCs because groups of neighboring wires are ganged together to make read-out feasible [**?**]. Since the hit uncertainties loosely distinguish between different types of hits, error propagation in Equation 4 is crucial: we must align to the weighted mean, rather than the unweighted mean.

The goal of track-based alignment is to measure the positions of each chamber with a better precision than the intrinsic resolution. We will treat each chamber as a rigid body; layers and superlayers have been firmly locked in place. However, the positions of internal elements may differ from their design geometry, so we will use measurements of DT layers and superlayers provided by the DT alignment group [**?**] and CSC layers from the CSC alignment group [**?**]. Additionally, we will refine the CSC layer determination with a special

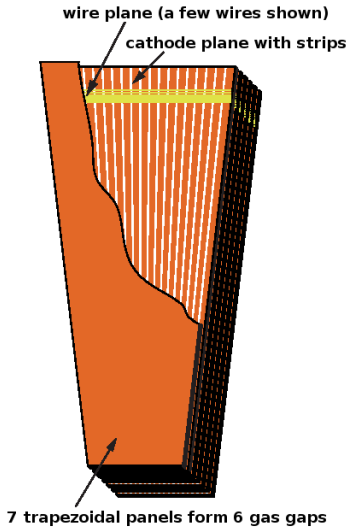

Figure 2: A CSC chamber: cathode strips measure the local x direction (global $r\phi$) and wire groups measure the local y direction (global r).

track-based alignment run, described below.

DT and CSC chambers are allowed to slide and rotate when the 4 T magnetic field turns on and off (several millimeters in the CSC case), to protect their internal structure from stresses from the enormous force of the field [**?**]. Therefore, chamber positions are always treated as floating parameters. Additionally, the DT chambers are mounted on 5 free-standing wheels and the CSC chambers are mounted on 4 free-standing disks for each endcap (total of 8). These can slide open and closed (on air and grease pads) to provide access to CMS's inner detectors. As a result, the wheels and disks are a source of correlated alignment error, observed to be as large as 7 mm. To avoid individually aligning all chambers on a wheel or disk by what is really a combined motion (for instance, 7 mm to the left), we will first align the wheels and disks as units, followed by the chambers.

2 General configuration and organization of studies

2.1 Nominal alignment procedure

In this section, we describe the nominal procedure that is used as a standard of comparison for systematics studies. The nominal procedure is not necessarily the best procedure: in the course of our studies, we find improvements on our initial best guess and present the optimal procedure at the end of each section as a recommendation.

The nominal procedure is conducted in two parts: first we align the barrel wheels and endcap disks relative to the CMS silicon tracker, then we align the individual chambers, also using the silicon tracker as a reference. We studied relative alignment of muon chambers without an external reference, but present that in a later section. We also discuss procedures for CSC layer alignment (the third alignment step) in its own section.

Component	x (cm)	y (cm)	z (cm)	ϕ_x (mrad)	ϕ_y (mrad)	ϕ_z (mrad)
Barrel wheels	1	1	1	1	1	1
DT chambers	0.3	0.3	0.3	1	1	1
Endcap disks	1	1	1	1	1	1
CSC chambers	0.3	0.3	0.3	1	1	1
CSC layers	0.0190	0.0340	0	0	0	0.040

Figure 3: Standard deviations of the Gaussians used to generate misalignments as a starting point for alignment studies. Values for CSC layers come from measurements of a subset with cosmic rays; the rest are conservative estimates.

Nominal alignment requires a source of high-p_T muons from the 14 TeV p-p collision vertex. We assume that the rate of this source is the rate of $W \to \mu\nu$ and $Z \to \mu\mu$ muons (effectively 6.6 nb and 0.5 nb, respectively, when branching fractions and acceptance are included) in collisions at 2×10^{32} /cm^2/s luminosity (0.2 nb^{-1}/s). In our simulations, we only generate $Z \to \mu\mu$ muons, and extrapolate to equal numbers of muon tracks. In a later section, we explore the effects of aligning with inclusively-selected muons and larger samples of lower-p_T muons. We also postpone discussions of alignments with other sources, such as beam-halo muons from the accelerator, and the results from cosmic ray alignments to a later section.

2.2 Initial conditions: the misalignment scenario

To study our alignment procedure in Monte Carlo, we must begin with a realistically misaligned detector. Wheels, disks, chambers, and CSC layers are misaligned once by random translations and rotations at the beginning of the alignment process, drawn from Gaussian distributions. Subdetectors, such as chambers on a wheel or disk, or layers in a chamber, are displaced relative to the displaced superstructure, thereby introducing correlations among subdetectors on the same superstructure. The standard deviations of the Gaussians used to generate misalignments are given in Table 3. Most values are conservative estimates, the exception being the magnitudes for CSC layers, taken from measurements with cosmic rays [**?**]. These misalignments are all larger than the 10 pb^{-1} projection (Muon10InvPbScenario) used for misalignment studies in physics analyses.

We align the muon system relative to the silicon tracker by extrapolating tracks from the tracker to the muon system. This makes the muon alignment resolution dependent on the tracker misalignment, a dependence which we will quantify. For the nominal procedure, we use the short-term tracker misalignment scenario intended for misalignment studies in physics analyses (TrackerShortTermScenario).

2.3 Track refitting procedure

At each iteration of the HIP algorithm, tracks selected for alignment are refit (from the outermost hits inward) under the current alignment conditions. This allows misalignments and alignment corrections to be propagated into the residual distributions, as residuals are calculated from the tracks' intersections with the assumed positions of the detector planes. We also have the opportunity to reweight the hits used in the track fit through the detectors' alignment parameter errors (APEs). The inverse weight of each hit (σ_r in Equation 1) is given by

$$\sigma_r{}^2 = \sigma_{\text{track}}{}^2 + \sigma_{\text{hit}}{}^2 + \sigma_{\text{APE}}{}^2 \tag{5}$$

where σ_{track} is the uncertainty in the track projection, σ_{hit} is the intrinsic hit uncertainty, and σ_{APE} is the alignment parameter error.

To decouple track-fitting from alignment, we severely deweight the hits in the muon system by giving them each a σ_{APE} of 10 cm. Track fits are thus dominated by the silicon tracker, but muon chamber residuals are still calculated and track fits are still sensitive to large kinks from multiple scattering. With this technique, alignment reaches its final accuracy in one iteration, because the fitted positions of tracks are largely undisturbed by moving the muon chambers.

It is important to verify that the optimum placement of muon chambers is not a function of σ_{APE}. For instance, we might imagine that one detector geometry optimizes residual distributions when muon hits are insignificant in the track-fit, and another geometry optimizes residual distributions in standard track reconstruction. We check for this by decreasing σ_{APE} from 10 cm to a negligible value, superexponentially with iteration number (according to

$$\sigma_{\text{APE}} = (10\text{ cm})\,\exp\left(-\frac{i^3}{10}\right) \tag{6}$$

where i is the number of completed iterations). After three iterations, σ_{APE} falls below σ_{hit} and track reconstruction becomes equivalent to the standard offline reconstruction algorithm (see Figure 4). As we will later see, aligned positions after the fourth iteration are the same as aligned positions in the first three iterations, validating our procedure.

2.4 Software framework

CommonAlignment, AlignmentProducer, HIPAlignmentAlgorithm [**?**]; CommonAlignment-Monitor, AlignmentMonitorMuonHIP, muonHIP.py [**?**]

3 Wheel and disk alignment

In a wheel/disk alignment, the alignment parameters are all expressed in global coordinates: x is parallel to the floor in the CMS cavern, y points upward, and z is along the beamline. The most sensitive parameter is ϕ_z, rotation around the beamline, since this corresponds to the most sensitive measurement dimension in all chambers. It is also the most relevant for accurately reconstructing muon p_T.

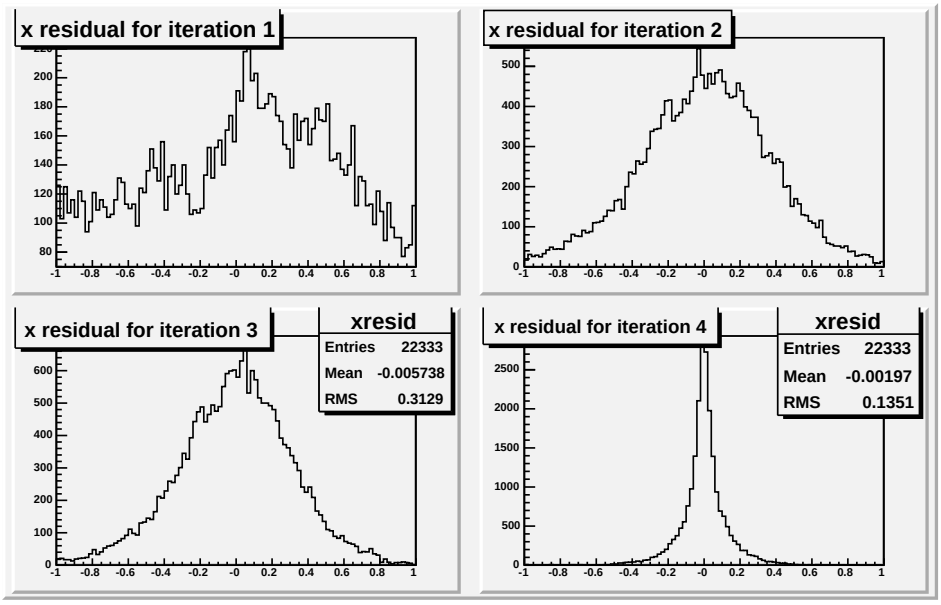

Figure 4: Residual distributions (*not* weighted by $1/{\sigma_r}^2$) in the first four iterations of a wheel/disk alignment, illustrating the transition from σ_{APE}-dominated track fits in the first three iterations to standard reconstruction from iteration 4 onward.

The second-most sensitive parameters are x and y. The x alignment is dominated by the chambers on the top and bottom of each wheel/disk, and y is dominated by chambers on the sides because the local x measurements of each chamber are better than the local y measurements. Wheels are directly sensitive to their z positions, but disks are only sensitive through imprecise local y measurements times $\cot\theta$, where θ is the azimuthal angle of the tracks with respect to the beamline. In the nominal wheel/disk alignment, only x, y, and ϕ_z are allowed to float.

3.1 Nominal results and consistency checks

The left-hand plot of Figure 5 presents the result of a typical wheel/disk alignment: ϕ_z for each of the 13 wheels and disks starts with an $\mathcal{O}(1$ mrad) misalignment and is brought within $\mathcal{O}(0.2$ mrad) of the correct alignment in the first iteration. The geometry doesn't change significantly between iterations 3 and 4, so the alignment is not dependent on σ_{APE}.

In this simulation and most alignment simulations presented in this note, the correct geometry that the alignment procedure should tend toward is the ideal, or design geometry of the detector. The same is not necessarily true in real alignments with data. To be sure that the alignment procedure is not artificially tending toward the ideal geometry, we rotated the tracker by 1 mrad, making the correct geometry for each wheel and disk offset from ideal by a 1 mrad ϕ_z rotation. The result of this test is presented on the right-hand side of Figure 5. All of the wheels and disks correctly tend toward 1 mrad instead of 0.

Thirteen wheels and disks is not a sufficiently large statistical sample to determine the accuracy of the alignment procedure. We therefore repeat the exercise 10 times with different

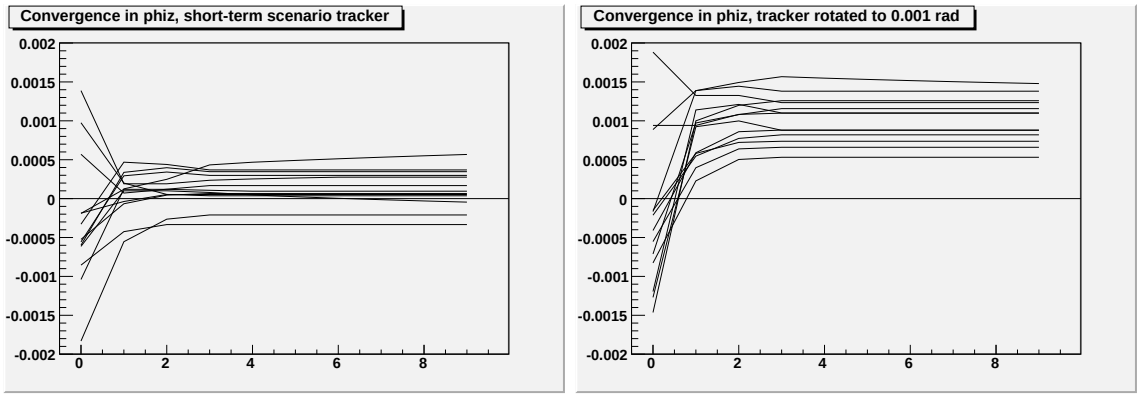

Figure 5: Left: convergence of ϕ_z as a function of iteration. Right: a simulation with the tracker rotated 1 mrad.

random starting positions for all wheels, disks, chambers, and CSC layers in each trial. (The tracker alignment is the same in each trial.) The positions of 13×10 aligned detectors are histogrammed, fit, and tabulated in Figure 6. Resolution in x and y is 1.31 ± 0.12 mm and resolution in ϕ_z is 0.20 ± 0.02 mrad. We prefer this method for determining alignment resolutions over the precision calculated by Equation 2, which assumes correct track fits (no tracker misalignment) and depends strongly on one's choice of $\sigma_{\rm APE}$.

3.2 Dependence on tracker alignment

Track-fits were provided by the silicon tracker, so it is natural to ask how muon alignment resolution depends on tracker misalignment. We repeated the above analysis (muon alignment in 10 trials) for an ideal tracker, twice the nominal short-term tracker misalignment, five times and ten times the tracker misalignment. This dependence is plotted in black in Figure 7: the tracker must be 3.8 times more misaligned than expected to degrade muon alignment by a factor of 2.

One might conjecture that the variance in the aligned positions of wheels and disks is dominated by internal misalignments: the misaligned chamber positions that our wheel/disk procedure cannot correct. In that case, the accuracy of ϕ_z is a function of the ratio of tracker misalignment to internal muon misalignment, and the latter was chosen ad-hoc! We therefore repeated the study with no internal misalignments in the muon wheels and disks, and found that the the curve is not greatly changed (plotted in red in Figure 7). Since the nominal internal misalignments were conservative, the dependence of ϕ_z resolution on tracker misalignment is somewhere between the red curve and the black curve (closer to the black curve).

3.3 Required integrated luminosity

The wheel/disk alignment procedure requires very few muons to reach its final accuracy. Even with deweighted muon chambers, the track-by-track residual distribution is 3 mm wide (see iteration 3 in Figure 4). In principle, the wheel and disk positions can reach a 1 mm

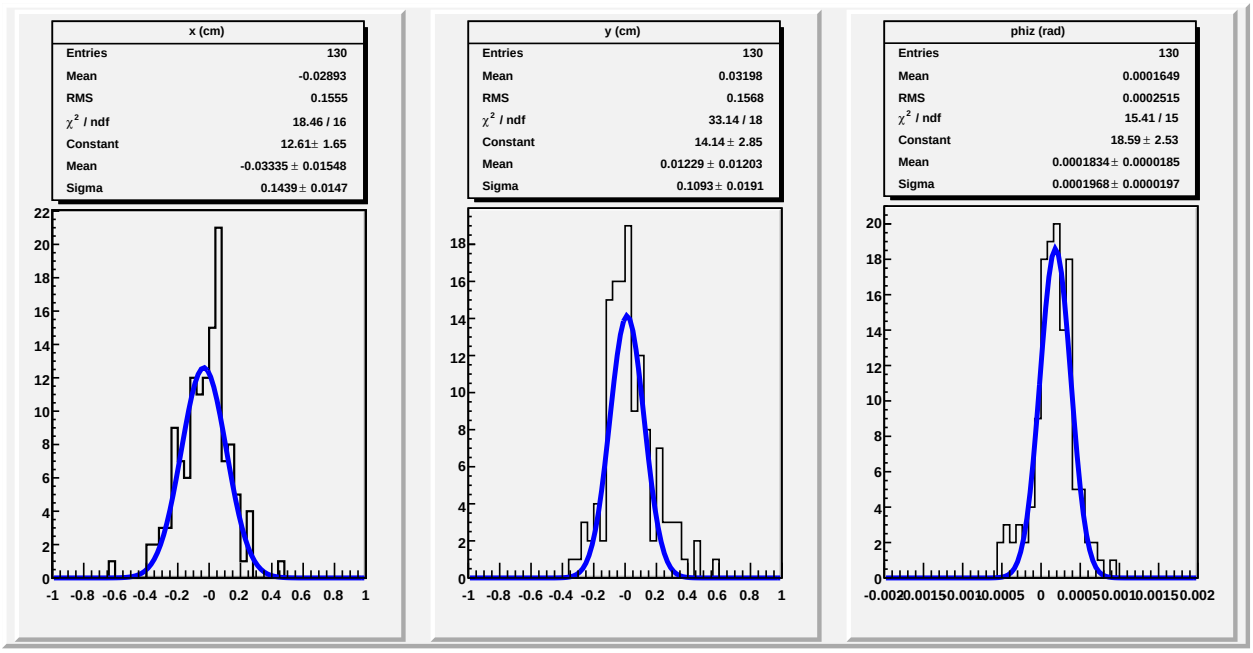

Figure 6: Aligned positions of all wheels and disks in 10 trials, randomizing the initial muon geometry with each trial.

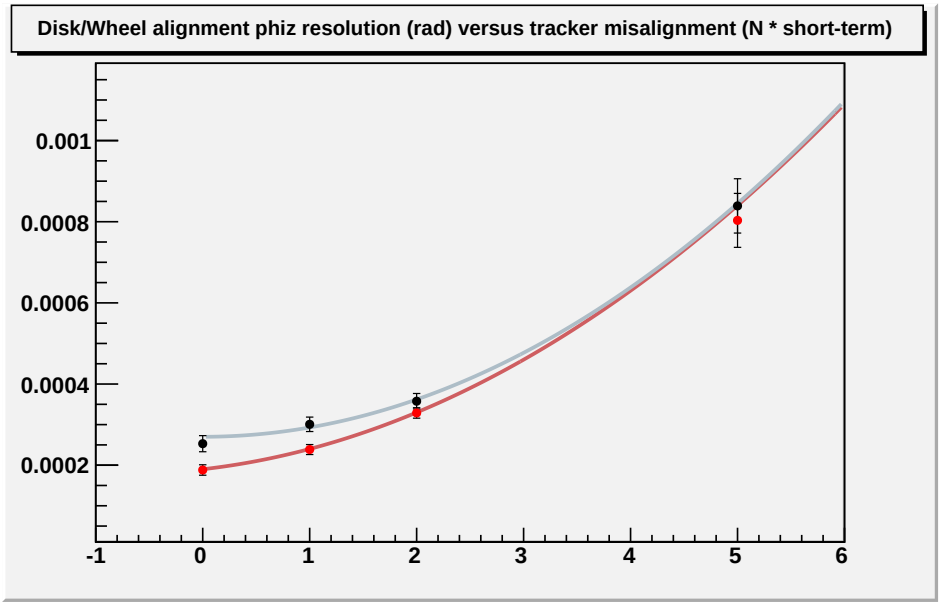

Figure 7: Dependence of muon alignment resolution on tracker misalignment, with (black) and without (red) internal misalignments (chambers and CSC layers). The horizontal axis is a scale factor applied to tracker misalignment: 0 is an ideal tracker and 1 is the nominal short-term scenario. The vertical axis is ϕ_z resolution.

accuracy with 10 tracks per detector, though 10 tracks aren't guaranteed to be optimally distributed in ϕ. We repeated the nominal procedure with 250, 500, 1000, and 2000 tracks, obtaining consistent results in each trial. To improve alignment beyond the millimeter scale, it is necessary to allow chambers to float.

3.4 Dependence on number of free parameters

The nominal procedure, in which only x, y, and ϕ_z are allowed to float in the alignment, is overly cautious. Three out of the eight superlayers in each barrel wheel measure the global z of hits directly, so we should at least let the z positions of wheels float. Moreover, ϕ_x and ϕ_y orientation can be determined from differences in z position between the top and bottom chambers (for ϕ_x) and the left and right chambers (for ϕ_y). We therefore get the best overall alignment by letting all 6 parameters float for barrel wheels and only 3 parameters (x, y, and ϕ_z) for endcap disks. Allowing more degrees of freedom for the disks degrades their z, ϕ_x, or ϕ_y alignment beyond the initial configuration without aiding the alignment of any other parameters.

In Figure 8, we present results for the 6-parameter wheel, 3-parameter disk alignment. The x and y resolutions are 0.71 $\pm$ 0.04 mm, z resolution is 0.89 $\pm$ 0.11 mm, ϕ_x and ϕ_y resolutions are 0.20 $\pm$ 0.02 mrad, and ϕ_z resolution is 0.11 $\pm$ 0.01 mrad.

3.5 Recommended wheel/disk alignment configuration

The 6-parameter wheel, 3-parameter disk alignment with at least 300 muons and 1 or 2 iterations is our recommended procedure for wheel and disk alignment. (The second iteration improves resolution by about 5%.) In early data, we will want to repeat some of the above tests to make sure that data behaves as well as Monte Carlo.

4 Chamber-by-chamber alignment

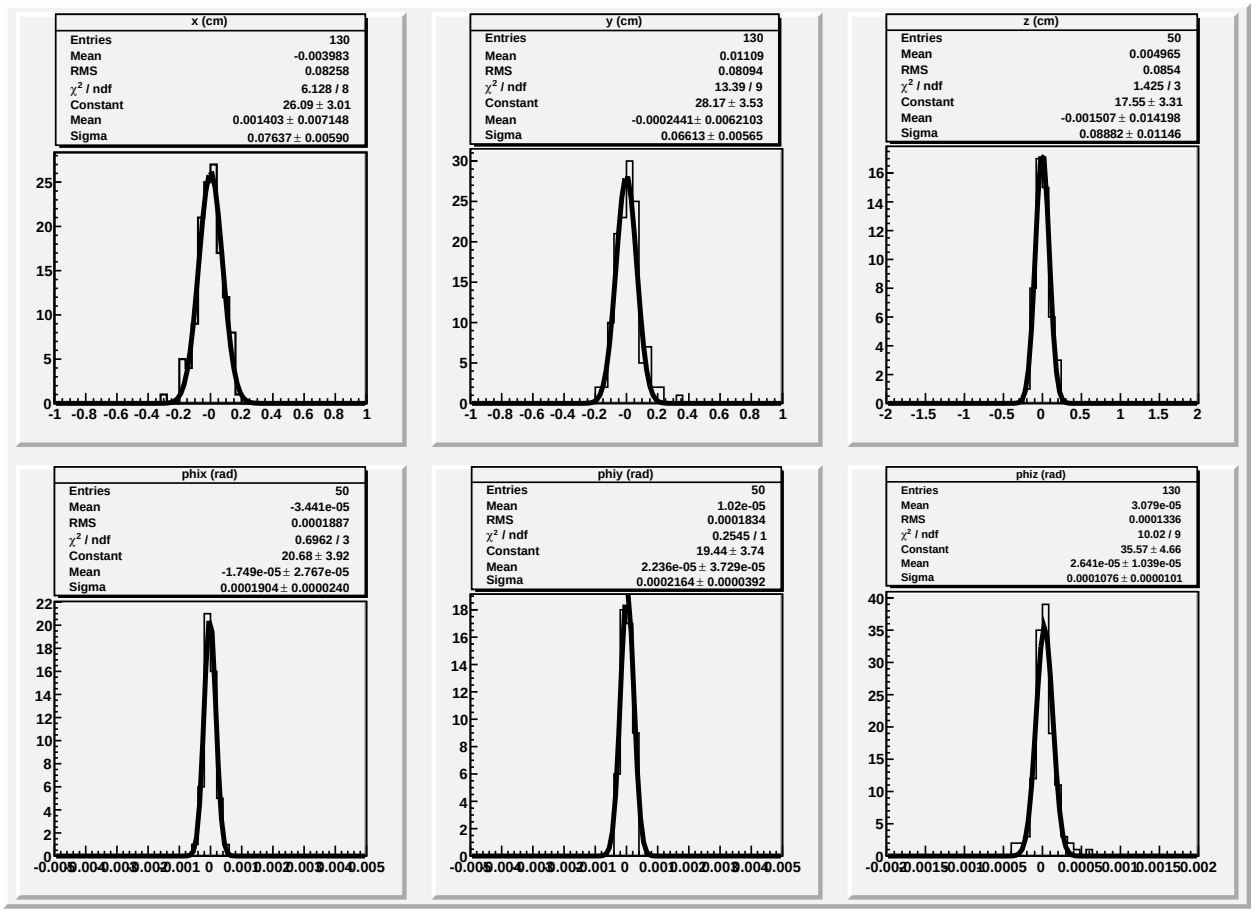

Figure 8: Optimal wheel/disk alignment, in which all 6 parameters float for barrel wheels but only x, y, and ϕ_z for endcap disks. Note that 13 alignables $\times$ 10 trials are presented for x, y, and ϕ_z, but only 5 alignables $\times$ 10 trials for z, ϕ_x, and ϕ_y.

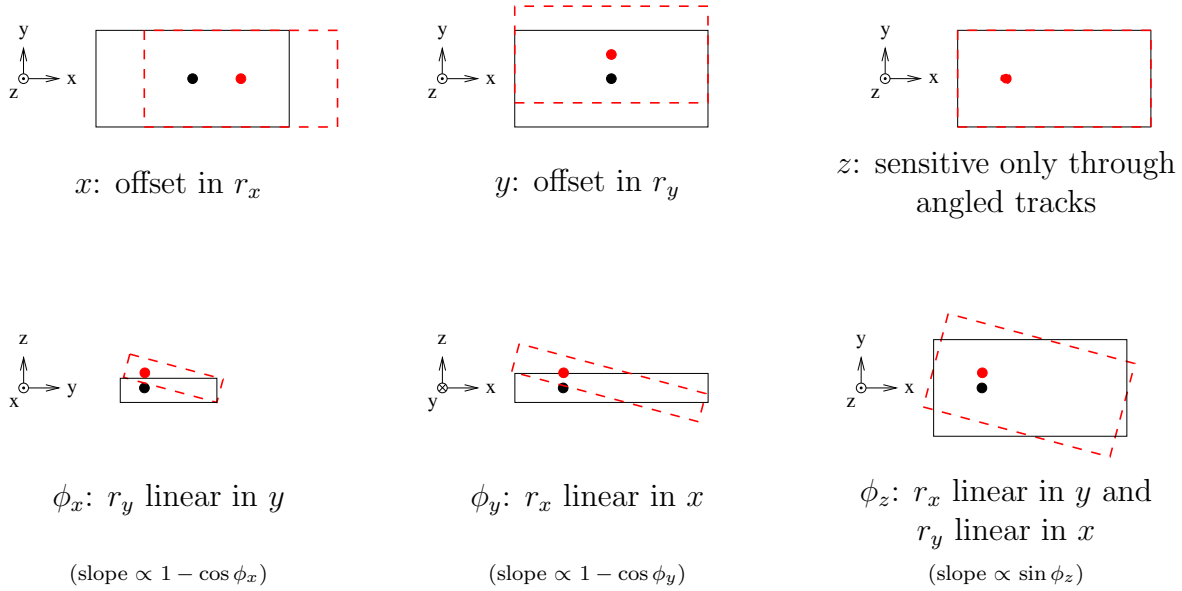

Figure 9: The relationship between chamber degrees of freedom and trends in the residuals distriutions (r_x and r_y versus local x and y coordinates of the track impact point). Dependence on z, ϕ_x, and ϕ_y is weak.

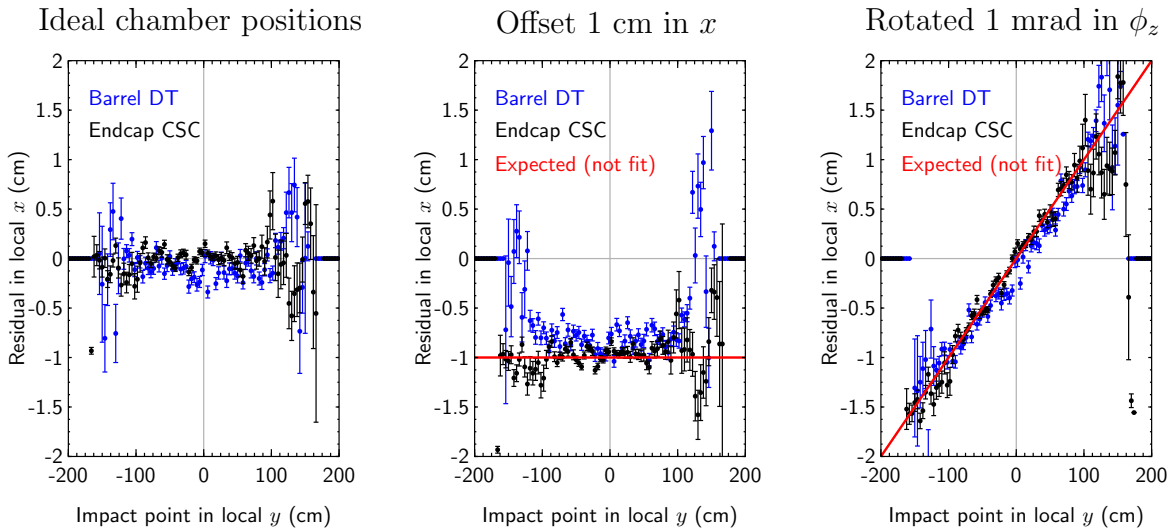

Figure 10: Demonstration of the trends presented in Figure 9 with coherently misaligned chambers.

5 ——— Old organization below this line; not necessarily consistent with new organization ———

6 Nominal procedure

We will first describe the nominal alignment procedure. This is the procedure by which routine alignment corrections are obtained, and the point of comparison for systematics studies.

6.1 Wheel and disk granularity

The first step in the procedure, as explained above, is to align the largest level of granularity: wheels in the barrel and disks in the endcap.

6.2 Chamber-by-chamber

default, standard of comparison

10 pb^{-1} of high p_T tracks (from Z's and W's)

number of hits cuts on tracks, pull cut on hits

Initial misalignment: the Muon10InvPbScenario with residual layer misalignments (to be determined from layer alignment studies)

chamber-by-chamber (CSC and DT) x, phiy, phiz float? can we relax this, letting y and phix float, too? Not for DT station 4, of course...

globalMuon APE scheme: starts large, descends rapidly, converges in a few iterations

standAloneMuon APE scheme: less steep, but relevant

7 Accuracy and Precision

output alignment parameter uncertainties (are they broken? why are they ∼4 times too big?): do they scale with residual misalignment?

if not, is there any other way to identify chambers with poor convergence? do they have fewer hits?

8 Performance issues

How does this scale with number of tracks (convert to pb^{-1} of W, Z, and if possible, a generic muon sample with a cut)

How much computer time does this take? (per iteration, and how many iterations are necessary?)

9 Special alignments

9.1 Quick disk alignment

how much data do we need to do this if the chambers and layers are also misaligned? (With ideal chambers, it's very quick! :)

MC and MTCC (compare with known x = 7 mm, y = 1 mm in MTCC phase II)

9.2 CSC Layer alignments

what is the nominal procedure, what degrees of freedom can we align, and how much data do we need to do it?

MC and MTCC

this will probably include Karoly's work: his plots with our results overlaid

10 Beam halo alignment of CSC layers

will we have this before data-taking?

New information from Karoly: no problem for inner ring, outer ring may have 0.8 million muons, though heavily emphasizing the inner radius part

11 Systematics studies

11.1 Dependence on tracker alignment

How does the globalMuon strategy depend on tracker alignment? (Initial studies suggest that the dependence is *very* weak. Is there anything wrong with my studies?)

New information: it looks like my procedure is working. Dependence on tracker alignment is probably *very weak!* I need to pull this together into a coherent story, with plots.

11.2 Dependence on momentum

How does resolution depend on the momentum of the input tracks? Use J/ψs to do an alignment if you have enough; otherwise, just compare width of the residuals distributions.

11.3 Dependence on fitting parameters

What happens if we use different sets of fitting parameters? I don't see much difference yet, but I haven't tried dropping "y" degrees of freedom.

11.4 Correlation between alignment and calibration

How well does alignment fare if we have a miscalibrated detector?

11.5 "Dependence on tracking algorithm"

11.5.1 Uncertainty in material distribution

Change the distribution of material in track-fitting but not in SimHit generation to simulate incorrect material description

11.5.2 Uncertainty in magnetic field

Same for magnetic field modeling

11.5.3 Dependence on track charge

How does alignment differ between positive and negative tracks? Can we cancel the effect by requiring equal populations?

11.5.4 Depdence on the actual algorithm used in tracking

If I'm very adventurous, I may try plugging in different tracking algorithms. I don't know how easy that is.

11.6 Background studies

Align with realistic backgrounds from CSA07

What are the optimized track quality cuts?

12 Conclusion

It works very, very, very well.